

Diagrammatic analysis of the Hellmann-Feynman theorem

R. Sartor

University of Liege, Institute of Physics B5, B-4000 Liege-1, Belgium

(Received 5 June 2000; published 20 September 2000)

We investigate the diagrammatic content of the Hellmann-Feynman theorem applied to nuclear matter within the framework of the Brueckner-Bethe-Goldstone theory for various self-consistent choices of the auxiliary potential. We identify cases in which one implicitly generates diagrams which are at odds with the Bethe-Brandow-Petscheck theorem. We point out that similar problems also arise with the Brueckner-Landau definition of the mean field. Finally, we characterize the structure exhibited by the potential energy diagrams when expressed in terms of G matrices and we provide the corresponding diagram rules.

PACS number(s): 21.65.+f, 21.60.-n

I. INTRODUCTION

The Hellmann-Feynman theorem (HFT) states that if H_λ is a λ dependent Hamiltonian, then one has

$$\frac{\langle \Psi_\lambda | dH_\lambda / d\lambda | \Psi_\lambda \rangle}{\langle \Psi_\lambda | \Psi_\lambda \rangle} = \frac{dE_\lambda}{d\lambda}, \quad (1)$$

where

$$H_\lambda | \Psi_\lambda \rangle = E_\lambda | \Psi_\lambda \rangle. \quad (2)$$

By considering the ground state of the Hamiltonian

$$H_\lambda = T + \lambda V, \quad (3)$$

the HFT yields the following exact expression for the expectation value of the potential energy of the considered system:

$$\langle V \rangle \equiv \frac{\langle \Psi | V | \Psi \rangle}{\langle \Psi | \Psi \rangle} = \left(\frac{dE_\lambda}{d\lambda} \right)_{\lambda=1}, \quad (4)$$

where we have used a convention that we adopt throughout this paper: if no confusion can arise, the index λ will be suppressed when it is equal to 1. Hence in the above equation $|\Psi\rangle$ denotes the ground state of $H = T + V$.

In order to use Eq. (4) in practice, one has to replace E_λ by some approximation. In this paper, we specialize to nuclear matter and we consider E_λ calculated within the framework of the Brueckner-Bethe-Goldstone (BBG) theory which provides a diagrammatic expansion for E_λ written as $E_\lambda = \langle \Phi | H_\lambda | \Psi_\lambda \rangle / \langle \Phi | \Psi_\lambda \rangle$, where $|\Phi\rangle$ is the uncorrelated ground state (see Ref. [1], and references therein). This way of expressing the ground state energy only gives access to $\langle \Phi | V | \Psi \rangle / \langle \Phi | \Psi \rangle$, which should not be confused with $\langle V \rangle$; in particular (see below) these quantities require different diagram rules. As is well known, in the BBG theory, one has to introduce a so-called auxiliary potential U which is determined by imposing some self-consistency requirement. In Sec. II where both the continuous and standard choices for U are examined, we discuss the diagrammatic problems which might arise when the self-consistency requirement is imposed for each value of the parameter λ . In Sec. III, we consider the calculation of the kinetic energy expectation value. We discuss the diagrams yielded by the HFT when used either within a conserving approximation or directly. In

Sec. IV, we point out that problems similar to those discussed in Sec. II also appear in the Brueckner-Landau definition of the mean field felt by a nucleon in the nuclear medium. Our results are summarized in Sec. V. In the appendix, we use the HFT to characterize the structure of the $\langle V \rangle$ -diagrams when expressed in terms of G matrices and to derive the corresponding diagram rules.

II. CALCULATION OF THE POTENTIAL ENERGY EXPECTATION VALUE

Let us assume that we define the auxiliary potential self-consistently for each value of λ and that we use the Brueckner-Hartree-Fock (BHF) approximation for the ground state energy

$$E_\lambda \approx E_\lambda^{\text{BHF}} \quad (5)$$

with

$$E_\lambda^{\text{BHF}} = \sum_i n_i t_i + \frac{1}{2} \sum_{i,j} n_i n_j \langle ij | G_\lambda(\epsilon_{\lambda,i} + \epsilon_{\lambda,j}) | ij \rangle_A. \quad (6)$$

The notations we use are the following ones. The momentum, spin, and isospin of the single particle states are denoted by a single roman letter, e.g., $a \equiv (\mathbf{k}_a, \sigma_a, \tau_a)$; the subscript A refers to antisymmetrization; n_a is the occupation number of the single particle state a in the free Fermi gas

$$\begin{aligned} n_a &= 1 \quad \text{for } |\mathbf{k}_a| \leq k_F \\ &= 0 \quad \text{for } |\mathbf{k}_a| > k_F, \end{aligned} \quad (7)$$

where k_F is the Fermi momentum, t_a is the single particle kinetic energy

$$t_a = \frac{|\mathbf{k}_a|^2}{2m} \quad (8)$$

(we take $\hbar = 1$), and $\epsilon_{\lambda,a}$ is the total (i.e., kinetic plus potential) single particle energy

$$\epsilon_{\lambda,a} = t_a + U_{\lambda,a}, \quad (9)$$

where $U_{\lambda,a}$ is the auxiliary potential. We begin our discussion with the continuous auxiliary potential. Then, in the BHF approximation, we have

$$U_{\lambda,a} = \sum_r n_r \langle ar | G_\lambda(\epsilon_{\lambda,a} + \epsilon_{\lambda,r}) | ar \rangle_A \quad (10)$$

for all single particle states a .

Both Eqs. (6) and (10) involve the Brueckner reaction matrix $G_\lambda(W_\lambda)$ which satisfies the Bethe-Goldstone equation that we write as

$$G_\lambda(W_\lambda) = \lambda v + \lambda v \mathcal{P}_\lambda(W_\lambda) G_\lambda(W_\lambda) \quad (11)$$

with

$$\mathcal{P}_\lambda(W_\lambda) = \sum_{p,q} \frac{(1-n_p)(1-n_q) |pq\rangle \langle pq|}{W_\lambda - \epsilon_{\lambda,p} - \epsilon_{\lambda,q}}. \quad (12)$$

The formal solution of Eq. (11) is given by

$$G_\lambda(W_\lambda) = [1 - \lambda v \mathcal{P}_\lambda(W_\lambda)]^{-1} \lambda v. \quad (13)$$

From Eqs. (11) and (13), one finds

$$\begin{aligned} \frac{dG_\lambda(W_\lambda)}{d\lambda} &= \frac{1}{\lambda} G_\lambda(W_\lambda) + \frac{1}{\lambda} G_\lambda(W_\lambda) \mathcal{P}_\lambda(W_\lambda) G_\lambda(W_\lambda) \\ &\quad + G_\lambda(W_\lambda) \frac{d\mathcal{P}_\lambda(W_\lambda)}{d\lambda} G_\lambda(W_\lambda). \end{aligned} \quad (14)$$

Because of the last term, Eq. (14) does not yield $dG_\lambda(W_\lambda)/d\lambda$ explicitly. Indeed, one has

$$\begin{aligned} \frac{d\mathcal{P}_\lambda(W_\lambda)}{d\lambda} &= - \sum_{p,q} \frac{(1-n_p)(1-n_q) |pq\rangle \langle pq|}{(W_\lambda - \epsilon_{\lambda,p} - \epsilon_{\lambda,q})^2} \\ &\quad \times \left(\frac{dW_\lambda}{d\lambda} - \frac{d\epsilon_{\lambda,p}}{d\lambda} - \frac{d\epsilon_{\lambda,q}}{d\lambda} \right) \end{aligned} \quad (15)$$

which involves the derivative of the reaction matrix through the derivatives of the single particle energies

$$\frac{d\epsilon_{\lambda,a}}{d\lambda} = \sum_r n_r \langle ar | \frac{dG_\lambda(\epsilon_{\lambda,a} + \epsilon_{\lambda,r})}{d\lambda} | ar \rangle_A, \quad (16)$$

where the right-hand side should be calculated using Eq. (14). This implies that the derivative of the single particle energies will contain G matrices to all powers. For the moment, we discard the contributions of third and higher powers, i.e., we use

$$\begin{aligned} \frac{d\epsilon_{\lambda,a}}{d\lambda} &\simeq \frac{1}{\lambda} \sum_r n_r \langle ar | G_\lambda(\epsilon_{\lambda,a} + \epsilon_{\lambda,r}) | ar \rangle_A \\ &\quad + \frac{1}{\lambda} \sum_r n_r \langle ar | G_\lambda(\epsilon_{\lambda,a} + \epsilon_{\lambda,r}) \mathcal{P}_\lambda(\epsilon_{\lambda,a} + \epsilon_{\lambda,r}) \\ &\quad \times G_\lambda(\epsilon_{\lambda,a} + \epsilon_{\lambda,r}) | ar \rangle_A. \end{aligned} \quad (17)$$

Taking Eqs. (4), (5), (6), (14), and (15) into account, one sees that this approximation for the single particle energy

derivatives amounts to calculating $\langle V \rangle$ up to terms of order G^4 . A straightforward calculation yields $\langle V \rangle$ as a sum of six terms

$$\langle V \rangle = \sum_{i=1}^6 V_i \quad (18)$$

with

$$V_1 = \frac{1}{2} \sum_{i,j} n_i n_j \langle ij | G(\epsilon_i + \epsilon_j) | ij \rangle_A, \quad (19)$$

$$V_2 = \frac{1}{4} \sum_{i,j,p,q} \frac{n_i n_j (1-n_p)(1-n_q)}{\epsilon_i + \epsilon_j - \epsilon_p - \epsilon_q} |\langle pq | G(\epsilon_i + \epsilon_j) | ij \rangle_A|^2, \quad (20)$$

$$\begin{aligned} V_3 &= - \frac{1}{2} \sum_{i,j,p,q,r} \frac{n_i n_j n_r (1-n_p)(1-n_q)}{(\epsilon_i + \epsilon_j - \epsilon_p - \epsilon_q)^2} \\ &\quad \times |\langle pq | G(\epsilon_i + \epsilon_j) | ij \rangle_A|^2 \langle jr | G(\epsilon_j + \epsilon_r) | jr \rangle_A, \end{aligned} \quad (21)$$

$$\begin{aligned} V_4 &= \frac{1}{2} \sum_{i,j,r,p,q} \frac{n_i n_j n_r (1-n_p)(1-n_q)}{(\epsilon_i + \epsilon_j - \epsilon_p - \epsilon_q)^2} \\ &\quad \times |\langle pq | G(\epsilon_i + \epsilon_j) | ij \rangle_A|^2 \langle qr | G(\epsilon_q + \epsilon_r) | qr \rangle_A, \end{aligned} \quad (22)$$

$$\begin{aligned} V_5 &= - \frac{1}{4} \sum_{i,j,r,p,q,s,t} \frac{n_i n_j n_r (1-n_p)(1-n_q)(1-n_s)(1-n_t)}{(\epsilon_i + \epsilon_j - \epsilon_p - \epsilon_q)^2 (\epsilon_j + \epsilon_r - \epsilon_s - \epsilon_t)} \\ &\quad \times |\langle pq | G(\epsilon_i + \epsilon_j) | ij \rangle_A|^2 |\langle st | G(\epsilon_j + \epsilon_r) | jr \rangle_A|^2, \end{aligned} \quad (23)$$

$$\begin{aligned} V_6 &= \frac{1}{4} \sum_{i,j,r,p,q,s,t} \frac{n_i n_j n_r (1-n_p)(1-n_q)(1-n_s)(1-n_t)}{(\epsilon_i + \epsilon_j - \epsilon_p - \epsilon_q)^2 (\epsilon_q + \epsilon_r - \epsilon_s - \epsilon_t)} \\ &\quad \times |\langle pq | G(\epsilon_i + \epsilon_j) | ij \rangle_A|^2 |\langle st | G(\epsilon_q + \epsilon_r) | qr \rangle_A|^2. \end{aligned} \quad (24)$$

The term V_1 comes from the first term of Eq. (14). This is the BHF contribution to $\langle V \rangle$. It is represented by diagram (a) in Fig. 1.

The term V_2 comes from the second term of Eq. (14). It is represented by diagram (b) in Fig. 1. This diagram looks spurious because it contains two successive G matrices linked by two particle lines. As explained in the Appendix, this peculiar feature stems from the diagram rules pertaining to $\langle V \rangle$. Diagram (b) is perfectly correct, it does not result from a double counting error.

The term V_3 is obtained by taking into account the first term of Eq. (17) to calculate the derivative of W_λ contained [see Eq. (15)] in the third term of Eq. (14). It is represented by diagram (c) in Fig. 1. One should note that the bubble is calculated on the energy shell. This is in keeping with the Bethe-Brandow-Petscheck (BBP) theorem [2] which is thus embodied in the HFT when we impose the self-consistency on the auxiliary potential for each value of the parameter λ . However, one might wonder why one obtains a contribution

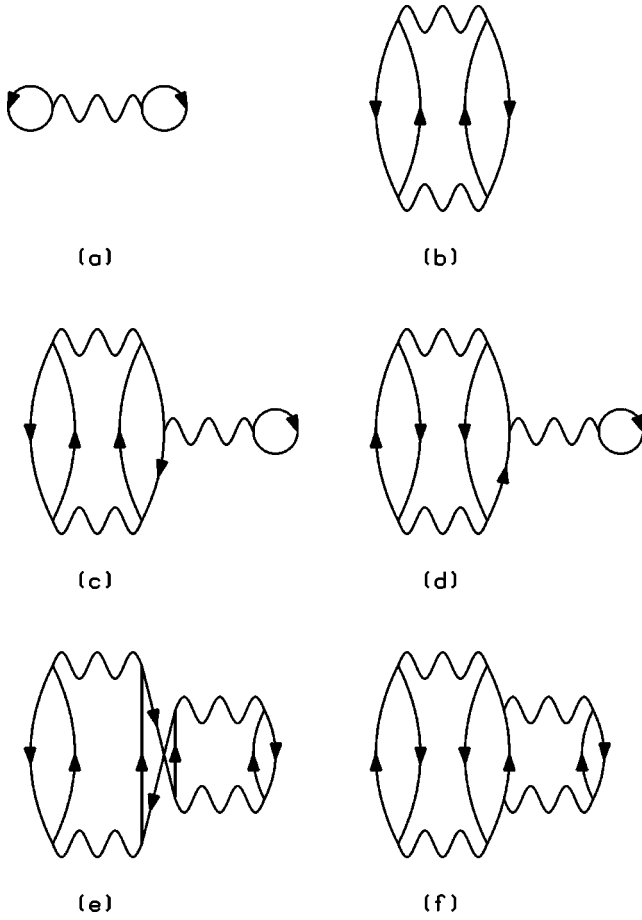


FIG. 1. Diagrammatic representation of Eq. (18). Wiggly lines represent antisymmetrized G matrices. Up and down going lines represent particle and hole states, respectively.

such as diagram (c) for $\langle V \rangle$ whereas for the binding energy E this diagram exactly cancels with the diagram obtained by replacing the bubble with a U insertion (see Fig. 2). This is again due to the diagram rules for $\langle V \rangle$. Actually, when considered as contributions to $\langle V \rangle$, diagrams (a) and (b) of Fig. 2 appear with extra weighting factors 3 and 2, respectively (see the Appendix), and as a consequence a copy of diagram (a) survives the cancellation process.

The term V_4 is obtained by taking into account the first term of Eq. (17) to calculate the derivatives of $\epsilon_{\lambda,p}$ and $\epsilon_{\lambda,q}$ contained [see Eq. (15)] in the third term of Eq. (14). It is

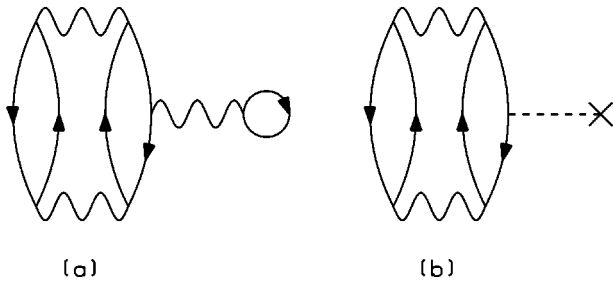


FIG. 2. Two contributions to the binding energy which compensate each other when the auxiliary potential (represented by a cross) is chosen self-consistently in the BHF approximation.

represented by diagram (d) in Fig. 1. One should note that the bubble is again calculated on the energy shell. This is a problem however since the BBP theorem does not apply to bubbles inserted on particle lines. A discussion of this point will be given below.

The term V_5 is obtained by taking into account the second term of Eq. (17) to calculate the derivative of W_λ contained [see Eq. (15)] in the third term of Eq. (14). It is represented by diagram (e) in Fig. 1. The insertion which appears on the right-hand side of the diagram has two successive G matrices linked by two particle lines. As for diagram (b), this just stems from the diagram rules pertaining to $\langle V \rangle$. One should also note that the BBP theorem is properly applied to this insertion.

The term V_6 is obtained by taking into account the second term of Eq. (17) to calculate the derivatives of $\epsilon_{\lambda,p}$ and $\epsilon_{\lambda,q}$ contained [see Eq. (15)] in the third term of Eq. (14). It is represented by diagram (f) in Fig. 1. Note that the two right-most G -matrices are calculated on the energy shell although the BBP does not apply.

Thus except for the contributions represented by diagrams (d) and (f) in Fig. 1, the HFT yields results which could have been obtained by directly applying the diagram rules pertaining to $\langle V \rangle$ in conjunction with the BBP theorem. We now show that the presence of diagrams (d) and (f) does not indicate that the HFT goes beyond the conventional rules. First, let us note that these diagrams are coming from the particle part of $d\mathcal{P}_\lambda/d\lambda$, i.e., from the part corresponding to $d(\epsilon_{\lambda,p} + \epsilon_{\lambda,q})/d\lambda$ in Eq. (15). Let us also remark that if we had not truncated the derivatives of the single particle energies at the order G^2 , we would have obtained not two but an infinite set of diagrams with G matrices improperly on the energy shell. As can easily be seen from Eqs. (1), (5), (6), and (14), the sum of all the diagrams in this set is given by

$$D_{pp} = \frac{1}{2} \sum_{i,j} n_i n_j \langle ij | G_\lambda(\epsilon_{\lambda,i} + \epsilon_{\lambda,j}) \times \left(\frac{d\mathcal{P}_\lambda(\epsilon_{\lambda,i} + \epsilon_{\lambda,j})}{d\lambda} \right)_{pp} G_\lambda(\epsilon_{\lambda,i} + \epsilon_{\lambda,j}) | ij \rangle_A, \quad (25)$$

where we used the subscript pp to refer to the particle part of $d\mathcal{P}_\lambda/d\lambda$. A simple calculation then yields

$$D_{pp} = \frac{1}{2} \sum_{i,j,p,q} \frac{n_i n_j (1-n_p)(1-n_q)}{(\epsilon_{\lambda,i} + \epsilon_{\lambda,j} - \epsilon_{\lambda,p} - \epsilon_{\lambda,q})^2} \times |\langle pq | G_\lambda(\epsilon_{\lambda,i} + \epsilon_{\lambda,j}) | ij \rangle_A|^2 \frac{dU_{\lambda,q}}{d\lambda}. \quad (26)$$

Let us emphasize that up to now we have applied Eq. (1) with E_λ calculated in the BHF approximation given by Eq. (6). When we go beyond that approximation we encounter the diagram depicted in Fig. 3 whose contribution is given by

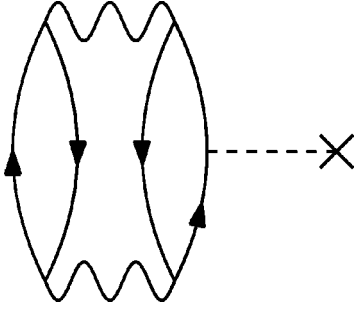


FIG. 3. Diagram used to exactly cancel an infinite series of diagrams in which the BBP theorem is wrongly applied. See text for details.

$$E_\lambda^U = -\frac{1}{2} \sum_{i,j,p,q} \frac{n_i n_j (1-n_p)(1-n_q)}{(\epsilon_{\lambda,i} + \epsilon_{\lambda,j} - \epsilon_{\lambda,p} - \epsilon_{\lambda,q})^2} \times |\langle pq | G_\lambda(\epsilon_{\lambda,i} + \epsilon_{\lambda,j}) | ij \rangle_A|^2 U_{\lambda,q} \quad (27)$$

with $U_{\lambda,q}$ as defined in Eq. (10). The derivative of E_λ^U is given by

$$\frac{dE_\lambda^U}{d\lambda} = -\frac{1}{2} \sum_{i,j,p,q} \frac{n_i n_j (1-n_p)(1-n_q)}{(\epsilon_{\lambda,i} + \epsilon_{\lambda,j} - \epsilon_{\lambda,p} - \epsilon_{\lambda,q})^2} \times |\langle pq | G_\lambda(\epsilon_{\lambda,i} + \epsilon_{\lambda,j}) | ij \rangle_A|^2 \frac{dU_{\lambda,q}}{d\lambda} + \dots, \quad (28)$$

where the ellipsis stands for the contributions coming from the G matrices contained in Eq. (27). One should note the extra minus sign which appears in this equation as compared to Eq. (26): this minus sign is responsible for the exact cancellation of D_{pp} , i.e., of the total contribution of the wrongly on the energy shell diagrams generated by applying the HFT with E_λ approximated by E_λ^{BHF} .

Although the approximation

$$E_\lambda \approx E_\lambda^{\text{BHF}} + E_\lambda^U \quad (29)$$

solves the problems stemming from the BHF approximation to E_λ , it will generate other wrongly on the energy shell contributions. These come from the derivatives of the G matrices contained in Eq. (27). It should be clear that these new wrong contributions will be exactly canceled by including diagrams with more U insertions in the calculation of E_λ and that this situation repeats itself ad infinitum. We believe that it is not sound to generate contributions to some quantity at a given approximation and to cancel them *exactly* in the next one. Therefore, we should avoid generating wrong diagrams from the beginning. To reach that goal, we simply observe that all the problems come from the λ dependence of the auxiliary potential. With a fixed U , the derivative of \mathcal{P}_λ vanishes identically and we are left with the first two terms on the right-hand side of Eq. (14). Then in the BHF approximation for E_λ , the HFT will only yield diagrams (a) and (b) of Fig. 1. Of course, the fixed auxiliary potential should be taken as the one corresponding to $\lambda = 1$. As we stated above, diagrams (c) and (e) in Fig. 1 are true contributions to $\langle V \rangle$

and this leads us to ask how they are generated since, in the fixed U context, the HFT with $E_\lambda \approx E_\lambda^{\text{BHF}}$ only yields diagrams (a) and (b) in Fig. 1. The answer to this question is provided by the diagrams in Fig. 2 whose sum does not vanish any more (except for $\lambda = 1$). A simple calculation shows that when their contributions are added to E_λ^{BHF} , one exactly retrieves diagrams (c) and (e) of Fig. 1. Note that if we just want to avoid wrong diagrams it is sufficient to work with a fixed potential for particle states while a λ dependent self-consistent auxiliary potential may be kept for hole states. Then, except for $\lambda = 1$, U_λ will display a gap at the Fermi momentum k_F . Let us just point out that close to the Fermi surface, the single particle energy of hole states will be above that of particle states when $\lambda < 1$ and one should take care of the vanishing energy denominators when one calculates the λ derivative.

Let us now consider the standard auxiliary potential which is taken as in Eq. (10) for hole states and is identified to 0 for particle states. From the discussion above it should be obvious that neither the λ dependent nor the λ independent standard auxiliary potentials will lead to any diagrammatic problems: all the diagrams generated by the HFT will be correct diagrams with the BBP theorem properly built-in. Again, diagrams such as diagrams (c) and (e) in Fig. 1 are generated by applying the HFT with $E_\lambda \approx E_\lambda^{\text{BHF}}$ if one uses the λ dependent standard U whereas one should take the contributions of the diagrams in Fig. 2 into account if one uses the λ independent standard U . The actual problem with the standard U is that the corresponding BBG expansion of the binding energy does not converge at the BHF level: one has to take the three hole line contributions into account [3–5]. As a consequence one expects that the corresponding approximation to $\langle V \rangle$ using the HFT will also be rather poor.

In the above discussion, particles and holes do not appear to play a symmetrical role. We did not find any problem stemming from the hole part of $d\mathcal{P}_\lambda/d\lambda$ i.e., from the part corresponding to $dW_\lambda/d\lambda$ in Eq. (15). This is only because we considered the BHF contribution to the auxiliary potential [see Eq. (10)]. In the terminology of [6] this is a contribution with crossed legs for hole states but not for particle states. Via the HFT, a contribution to U_λ with crossed legs will generate $\langle V \rangle$ diagrams containing insertions with crossed legs and vice versa [see, e.g., diagrams (c)–(f) in Fig. 1]. Since the BBP theorem only applies to insertions with crossed legs, this explains why in the BHF approximation to U_λ we had problems with insertions on particle lines only. These problems will also appear for insertions on hole lines if we take into account contributions to U_λ which are not with crossed legs for hole states. Conversely if we identify U_λ with the Brandow auxiliary potential [6], i.e., as the sum of all the insertions with crossed legs, the problems with the BBP theorem will disappear for both the hole and particle insertions. The Brandow auxiliary potential leads however to the same convergence problems as the standard auxiliary potential: the BBG expansion of the binding energy may not be truncated at the BHF level.

III. CALCULATION OF THE KINETIC ENERGY EXPECTATION VALUE

The exact expectation value of the kinetic energy is given by

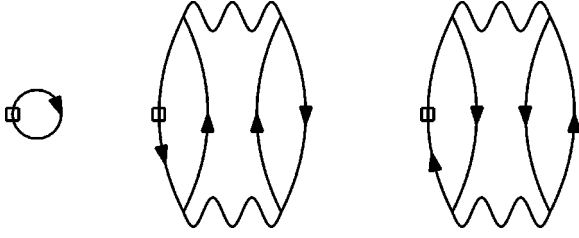


FIG. 4. Diagrammatic representation of Eq. (39). The squares represent kinetic energy insertions. The first diagram corresponds to the kinetic energy of the free Fermi gas.

$$\langle T \rangle \equiv \frac{\langle \Psi | T | \Psi \rangle}{\langle \Psi | \Psi \rangle} = E - \langle V \rangle \quad (30)$$

and it is tempting to use this equation to calculate approximations to $\langle T \rangle$. One would simply replace E by some approximation and $\langle V \rangle$ by the corresponding approximation obtained from the HFT. This is the procedure followed in Ref. [7]. It has the advantage to deal (by construction) with approximations to E , $\langle T \rangle$ and $\langle V \rangle$ which are conserving in the sense that Eq. (30) is satisfied. One should note however that in general such approximations to $\langle T \rangle$ cannot be represented by the usual Goldstone diagrams. Let us take for instance $E_\lambda \simeq E_\lambda^{\text{BHF}}$ and let us work with a λ independent auxiliary potential. The corresponding contribution to $\langle T \rangle$ will then be given by the free Fermi gas kinetic energy, which is represented by the first diagram in Fig. 4, minus the contribution of diagram (b) in Fig. 1. Except when one uses no auxiliary potential at all, the latter contribution cannot be written in terms of the usual kinetic energy diagrams which, like those depicted in Fig. 4, contain a kinetic energy insertion.

The usual kinetic energy diagrams can however be obtained by an application of the HFT independent of the one used for $\langle V \rangle$ [8]. We show this in detail. Let us multiply the mass of each nucleon by $1/\lambda$; this leads us to consider the following λ dependent Hamiltonian

$$H_\lambda = \lambda T + V. \quad (31)$$

The HFT then yields

$$\langle T \rangle = \left(\frac{dE_\lambda}{d\lambda} \right)_{\lambda=1}, \quad (32)$$

where E_λ is the ground state energy of the Hamiltonian of Eq. (31). For simplicity, let us work again in the BHF approximation with a λ independent auxiliary potential. Now, we have

$$E_\lambda^{\text{BHF}} = \lambda \sum_i n_i t_i + \frac{1}{2} \sum_{i,j} n_i n_j \langle ij | G_\lambda(\epsilon_{\lambda,i} + \epsilon_{\lambda,j}) | ij \rangle_A \quad (33)$$

with

$$G_\lambda(\epsilon_{\lambda,i} + \epsilon_{\lambda,j}) = v + v \mathcal{P}_\lambda(\epsilon_{\lambda,i} + \epsilon_{\lambda,j}) G_\lambda(\epsilon_{\lambda,i} + \epsilon_{\lambda,j}) \quad (34)$$

and

$$\begin{aligned} & \mathcal{P}_\lambda(\epsilon_{\lambda,i} + \epsilon_{\lambda,j}) \\ &= \sum_{p,q} \frac{(1-n_p)(1-n_q) |pq\rangle \langle pq|}{\lambda(t_i + t_j - t_p - t_q) + (U_i + U_j - U_p - U_q)}, \end{aligned} \quad (35)$$

where we have written the single particle energies as

$$\epsilon_{\lambda,a} = \lambda t_a + U_a. \quad (36)$$

For definiteness, we work with the continuous auxiliary potential so that the latter equation applies for all single particle states a .

The HFT will again involve the λ -derivative of the G matrix. Now, we have [compare with Eq. (14)]

$$\begin{aligned} & \frac{dG_\lambda(\epsilon_{\lambda,i} + \epsilon_{\lambda,j})}{d\lambda} \\ &= G_\lambda(\epsilon_{\lambda,i} + \epsilon_{\lambda,j}) \frac{d\mathcal{P}_\lambda(\epsilon_{\lambda,i} + \epsilon_{\lambda,j})}{d\lambda} G_\lambda(\epsilon_{\lambda,i} + \epsilon_{\lambda,j}) \end{aligned} \quad (37)$$

with

$$\begin{aligned} & \frac{d\mathcal{P}_\lambda(\epsilon_{\lambda,i} + \epsilon_{\lambda,j})}{d\lambda} \\ &= - \sum_{p,q} \frac{(1-n_p)(1-n_q) |pq\rangle \langle pq|}{(\lambda(t_i + t_j - t_p - t_q) + (U_i + U_j - U_p - U_q))^2} \\ & \quad \times (t_i + t_j - t_p - t_q). \end{aligned} \quad (38)$$

From Eqs. (32), (33), (37), and (38), one obtains

$$\begin{aligned} \langle T \rangle &= \sum_i n_i t_i - \frac{1}{2} \sum_{i,j,p,q} \frac{n_i n_j (1-n_p)(1-n_q)}{(\epsilon_i + \epsilon_j - \epsilon_p - \epsilon_q)^2} \\ & \quad \times t_i | \langle pq | G(\epsilon_i + \epsilon_j) | ij \rangle_A |^2 \\ & \quad + \frac{1}{2} \sum_{i,j,p,q} \frac{n_i n_j (1-n_p)(1-n_q)}{(\epsilon_i + \epsilon_j - \epsilon_p - \epsilon_q)^2} \\ & \quad \times t_p | \langle pq | G(\epsilon_i + \epsilon_j) | ij \rangle_A |^2. \end{aligned} \quad (39)$$

This expression is represented by the diagrams with kinetic energy insertions depicted in Fig. 4. Since in any contribution to E_λ , the parameter λ only multiplies the kinetic energy part of some single particle energy, it is clear that the results we have obtained in the BHF approximation generalize to any other approximation to E_λ : every contribution to $\langle T \rangle$ generated by using the HFT with the Hamiltonian of Eq. (31) will correspond to some usual kinetic energy diagram. The converse is also true: every usual kinetic energy diagram can be obtained from the contribution of some diagram pertaining to E_λ by means of the HFT. The latter diagram can be constructed from the considered kinetic energy diagram in the following way. First, suppress the kinetic energy insertion. If the resulting diagram does not contain two successive G matrices linked by particle lines, then it is the looked for

E_λ diagram. The HFT will give back the considered kinetic energy diagram when one calculates the λ derivative of the energy denominator corresponding to the former location of the kinetic energy insertion. If the diagram resulting from the suppression of the kinetic insertion contains two successive G matrices linked by particle lines, then one obtains the looked for E_λ diagram by collapsing these two successive G matrices into a single one. The HFT will give back the considered kinetic energy diagram when one calculates, via Eq. (37), the λ derivative of the G matrix which resulted from the collapse.

IV. THE BRUECKNER-LANDAU DEFINITION OF THE MEAN FIELD

In this section which is somewhat out of the main line of this paper, we point out that we might encounter problems similar to those of Sec. II if we define the mean field M_k felt by a nucleon in the nuclear medium, as the functional derivative of the binding energy with respect to the occupation number [9,10]

$$M_k = \frac{\delta E}{\delta n_k} - t_k. \quad (40)$$

Consider again the BHF approximation to E

$$E^{\text{BHF}} = \sum_i n_i t_i + \frac{1}{2} \sum_{i,j} n_i n_j \langle ij | G(\epsilon_i + \epsilon_j) | ij \rangle_A \quad (41)$$

with

$$G(\epsilon_i + \epsilon_j) = v + v \mathcal{P}(\epsilon_i + \epsilon_j) G(\epsilon_i + \epsilon_j) \quad (42)$$

and

$$\mathcal{P}(\epsilon_i + \epsilon_j) = \sum_{p,q} \frac{(1-n_p)(1-n_q) |pq\rangle \langle pq|}{\epsilon_i + \epsilon_j - \epsilon_p - \epsilon_q + i\eta}, \quad (43)$$

where the infinitesimal quantity $i\eta$ is responsible for the imaginary part of the mean field. It has been repeatedly emphasized (see, e.g., Chap. 6 in Ref. [1]) that the calculation of the mean field requires a continuous auxiliary potential. Hence in the BHF approximation, we should use

$$\epsilon_a = t_a + U_a \quad (44)$$

with

$$U_a = \sum_r n_r \langle ar | G(\epsilon_a + \epsilon_r) | ar \rangle_A \quad (45)$$

for all single particle states a . From Eqs. (40) and (42), one obtains

$$M_k \simeq \sum_j n_j \langle kj | G(\epsilon_k + \epsilon_j) | kj \rangle_A + \frac{1}{2} \sum_{i,j} n_i n_j \langle ij | \frac{\delta G(\epsilon_i + \epsilon_j)}{\delta n_k} | ij \rangle_A, \quad (46)$$

where

$$\frac{\delta G(\epsilon_i + \epsilon_j)}{\delta n_k} = G(\epsilon_i + \epsilon_j) \frac{\delta \mathcal{P}(\epsilon_i + \epsilon_j)}{\delta n_k} G(\epsilon_i + \epsilon_j). \quad (47)$$

Calculating the functional derivative of \mathcal{P} from Eq. (43) yields

$$\begin{aligned} \frac{\delta \mathcal{P}(\epsilon_i + \epsilon_j)}{\delta n_k} = & - \sum_q \frac{(1-n_q) |kq\rangle \langle kq|}{\epsilon_i + \epsilon_j - \epsilon_k - \epsilon_q + i\eta} \\ & - \sum_p \frac{(1-n_p) |pk\rangle \langle pk|}{\epsilon_i + \epsilon_j - \epsilon_p - \epsilon_k + i\eta} \\ & - \sum_{p,q} \frac{(1-n_p)(1-n_q) |pq\rangle \langle pq|}{(\epsilon_i + \epsilon_j - \epsilon_p - \epsilon_q)^2} \left(\frac{\delta \epsilon_i}{\delta n_k} + \frac{\delta \epsilon_j}{\delta n_k} \right) \\ & + \sum_{p,q} \frac{(1-n_p)(1-n_q) |pq\rangle \langle pq|}{(\epsilon_i + \epsilon_j - \epsilon_p - \epsilon_q)^2} \left(\frac{\delta \epsilon_p}{\delta n_k} + \frac{\delta \epsilon_q}{\delta n_k} \right). \end{aligned} \quad (48)$$

Since the auxiliary potential [see Eq. (45)] is also a functional of the occupation number one has

$$\frac{\delta \epsilon_a}{\delta n_k} = \langle ak | G(\epsilon_a + \epsilon_k) | ak \rangle_A + \sum_r n_r \langle ar | \frac{\delta G(\epsilon_a + \epsilon_r)}{\delta n_k} | ar \rangle_A. \quad (49)$$

Comparing with Eqs. (47) and (48), one sees that M_k will involve G matrices to all powers. This is of course reminiscent of a similar situation encountered in Sec. II. By only keeping terms up to order G^2 in $\delta \epsilon_a / \delta n_k$, i.e., by taking

$$\begin{aligned} \frac{\delta \epsilon_a}{\delta n_k} = & \langle ak | G(\epsilon_a + \epsilon_k) | ak \rangle_A + \sum_{r,q} \frac{n_r (1-n_q)}{\epsilon_a + \epsilon_r - \epsilon_k - \epsilon_q + i\eta} \\ & \times |\langle kq | G(\epsilon_a + \epsilon_r) | ar \rangle_A|^2, \end{aligned} \quad (50)$$

one easily finds that

$$M_k = \sum_{i=1}^6 M_{k,i} \quad (51)$$

with

$$M_{k,1} = \sum_j n_j \langle kj | G(\epsilon_k + \epsilon_j) | kj \rangle_A, \quad (52)$$

$$M_{k,2} = -\frac{1}{2} \sum_{i,j,q} \frac{n_i n_j (1-n_q)}{\epsilon_i + \epsilon_j - \epsilon_k - \epsilon_q + i\eta} |\langle kj | G(\epsilon_i + \epsilon_j) | ij \rangle_A|^2, \quad (53)$$

$$M_{k,3} = -\frac{1}{2} \sum_{i,j,p,q} \frac{n_i n_j (1-n_p)(1-n_q)}{(\epsilon_i + \epsilon_j - \epsilon_p - \epsilon_q)^2} |\langle pq | G(\epsilon_i + \epsilon_j) | ij \rangle_A|^2 |\langle ik | G(\epsilon_i + \epsilon_k) | ik \rangle_A, \quad (54)$$

$$M_{k,4} = \frac{1}{2} \sum_{i,j,p,q} \frac{n_i n_j (1-n_p)(1-n_q)}{(\epsilon_i + \epsilon_j - \epsilon_p - \epsilon_q)^2} |\langle pq | G(\epsilon_i + \epsilon_j) | ij \rangle_A|^2 \langle pk | G(\epsilon_p + \epsilon_k) | pk \rangle_A, \quad (55)$$

$$M_{k,5} = \frac{1}{2} \sum_{i,j,p,q,r,s} \frac{n_i n_j n_r (1-n_p)(1-n_q)(1-n_s)}{(\epsilon_i + \epsilon_j - \epsilon_p - \epsilon_q)^2 (\epsilon_i + \epsilon_r - \epsilon_k - \epsilon_s + i\eta)} |\langle pq | G(\epsilon_i + \epsilon_j) | ij \rangle_A|^2 |\langle ks | G(\epsilon_i + \epsilon_r) | ir \rangle_A|^2, \quad (56)$$

$$M_{k,6} = -\frac{1}{2} \sum_{i,j,p,q,r,s} \frac{n_i n_j n_r (1-n_p)(1-n_q)(1-n_s)}{(\epsilon_i + \epsilon_j - \epsilon_p - \epsilon_q)^2 (\epsilon_p + \epsilon_r - \epsilon_k - \epsilon_s + i\eta)} |\langle pq | G(\epsilon_i + \epsilon_j) | ij \rangle_A|^2 |\langle ks | G(\epsilon_p + \epsilon_r) | pr \rangle_A|^2. \quad (57)$$

The term $M_{k,1}$ is simply the first term of Eq. (46). This is the BHF contribution to M_k . It is represented by diagram (a) in Fig. 5.

The term $M_{k,2}$ comes from the contribution of the first two terms of Eq. (48) to the second term of Eq. (46). It is represented by diagram (b) in Fig. 5. This is the so-called Pauli rearrangement contribution to the mean field.

The term $M_{k,3}$ is obtained by using the first term of Eq. (50) to calculate the contribution of the third term of Eq. (48) to the second term of Eq. (46). It is represented by diagram (c) in Fig. 5. One should note that the middle G matrix is calculated on the energy shell. This is in keeping with the BBP theorem.

The term $M_{k,4}$ is obtained by using the first term of Eq. (50) to calculate the contribution of the fourth term of Eq. (48) to the second term of Eq. (46). It is represented by diagram (d) in Fig. 5. The middle G matrix is again calculated on the energy shell although the BBP theorem does not apply.

The term $M_{k,5}$ is obtained by using the second term of Eq. (50) to calculate the contribution of the third term of Eq. (48) to the second term of Eq. (46). It is represented by diagram (e) in Fig. 5. The BBP theorem is properly applied to the two leftmost G matrices.

The term $M_{k,6}$ is obtained by using the second term of Eq. (50) to calculate the contribution of the fourth term of Eq. (48) to the second term of Eq. (46). It is represented by diagram (f) in Fig. 5. The two leftmost G matrices are calculated on the energy shell although the BBP theorem does not apply.

Thus as in Sec. II, we have obtained two diagrams, namely diagrams (d) and (f), whose contributions cannot be calculated by means of the usual diagram rules pertaining to M_k . Once more, this is an artifact due to the approximation we used for the binding energy E . Indeed, if we take the

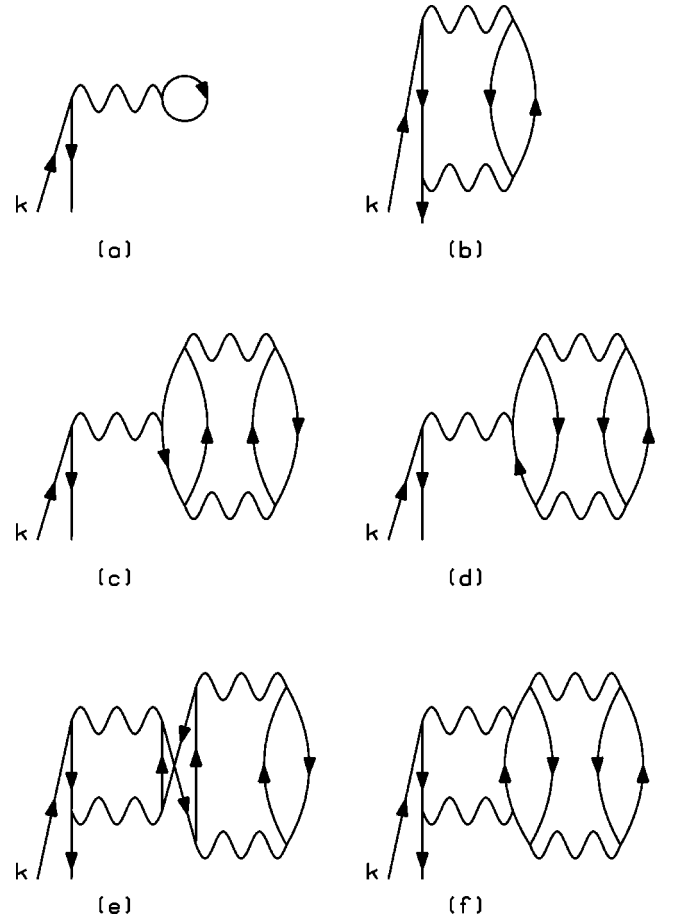


FIG. 5. Diagrammatic representation of Eq. (51). Although we always draw the external lines from below, the diagrams represent contributions to the mean field for both hole and particle states.

diagram of Fig. 3 into account to calculate E , we shall obtain an additional contribution to M_k given by

$$M_k^U = -\frac{1}{4} \sum_{i,j,p,q} \frac{n_i n_j (1-n_p)(1-n_q)}{(\epsilon_i + \epsilon_j - \epsilon_p - \epsilon_q)^2} \times |\langle pq | G(\epsilon_i + \epsilon_j) | ij \rangle_A|^2 \left(\frac{\delta \epsilon_p}{\delta n_k} + \frac{\delta \epsilon_q}{\delta n_k} \right) + \dots, \quad (58)$$

where the ellipsis stands for the contributions coming from the G matrices contained in the diagram. One notes that this cancels not only the contributions of diagrams (d) and (f) of Fig. 5 but also all the contributions we would have obtained from the fourth term of Eq. (48) if we had not truncated the functional derivative of the single particle energies at the order G^2 . Thus as in Sec. II, the wrong diagrams which are generated at some approximation level for E are exactly canceled at the next level. To avoid this (generation-exact cancellation) process, it suffices to use a fixed auxiliary potential, i.e., one without any functional dependence upon the occupation number n_k . In that case the diagrams (c) and (e) of Fig. 5 where the BBP is correctly applied will be generated by the functional derivative of the first diagram of Fig. 2.

V. SUMMARY

In this paper, we have discussed the implicit diagrammatic content of the HFT within the framework of the BBG theory. We have found that if one uses a λ dependent auxiliary potential, there are cases in which one generates diagrams where the BBP theorem is wrongly applied. We have shown that this is due to the fact that one has to use some approximation to the binding energy E_λ in order to apply the HFT in practice. The wrong diagrams can always be *exactly* canceled by improving the approximation to E_λ at the expense, however, of generating other wrong diagrams. This has led us to advocate the use of a λ independent auxiliary potential in order to retrieve a situation which is cleaner from a diagrammatic point of view. We have also discussed two distinct applications of the HFT to the calculation of the kinetic energy of nuclear matter $\langle T \rangle$. The usual kinetic energy diagrams, i.e., the diagrams with a kinetic energy insertion on a particle or a hole line cannot be obtained by using the HFT within the conserving definition of $\langle T \rangle$ except in the academic case in which one uses no auxiliary potential at all. Finally we have pointed out that analogous problems arise with the Brueckner-Landau definition of the mean field.

The following appendix extends the discussion of the $\langle V \rangle$ diagrams given in Ref. [11].

APPENDIX

In Ref. [11], the existence of diagrams such as diagram (b) in Fig. 1 was justified by directly resumming a series of $\langle V \rangle$ diagrams expressed in terms of the bare interaction v . We remind the reader that these diagrams are in one to one correspondence with those pertaining to the binding energy

E (more precisely with those pertaining to $E - T_F$ where T_F is the free Fermi gas kinetic energy) but that the diagram rules are different: to calculate the contribution of a $\langle V \rangle$ diagram containing n bare interactions, one has to multiply by n the contribution one obtains using the rules which would apply if it were an E diagram.

One can immediately convince oneself by considering other examples, that because of the extra weighting factor n , this direct resummation technique is rather inconvenient. In particular, it is hard to see what the general structure of the $\langle V \rangle$ diagrams will be when we express them in terms of G matrices. In addition, the corresponding diagram rules are not obvious. In this Appendix, we show how the HFT can be used to solve these problems in a straightforward manner. More precisely, we prove that the following properties hold.

Property 1. A spurious looking pair, i.e., two successive G matrices linked by two particle lines, can only appear once in a diagram.

Property 2. The contribution of a diagram containing a spurious looking pair is calculated as usual, i.e., by means of the diagram rules which apply to the E diagrams when they are expressed in terms of G matrices.

Property 3. The contribution of a diagram containing no spurious looking pair is obtained by multiplying the contribution calculated as usual, by the number of G matrices contained in the diagram.

Indeed, consider any E diagram $D(E;G)$ expressed in terms of G matrices. It is the sum of a series of E diagrams $D_i(E;v)$ expressed in terms of the bare interaction v :

$$D(E;G) = \sum_i D_i(E;v). \quad (A1)$$

Let us now consider the E diagrams $D_i(E;v)$ as $\langle V \rangle$ diagrams $D_i(V;v)$. The HFT gives

$$\begin{aligned} \sum_i D_i(V;v) &= \sum_i \left(\frac{dD_i(E;\lambda v)}{d\lambda} \right)_{\lambda=1} \\ &= \left(\frac{d}{d\lambda} \sum_i D_i(E;\lambda v) \right)_{\lambda=1} \\ &= \left(\frac{dD(E;G_\lambda)}{d\lambda} \right)_{\lambda=1} \end{aligned} \quad (A2)$$

with

$$G_\lambda(W) = \lambda v + \lambda v \mathcal{P}(W) G_\lambda(W), \quad (A3)$$

where

$$\mathcal{P}(W) = \sum_{p,q} \frac{(1-n_p)(1-n_q) |pq\rangle \langle pq|}{W - \epsilon_p - \epsilon_q}. \quad (A4)$$

Equations (A3) and (A4) should be compared with Eqs. (11) and (12): now neither W nor \mathcal{P} depend on λ because we use a fixed auxiliary potential. Note that in Eq. (A2), $D(E;G_\lambda)$ is just the contribution of the E diagram we started from with

each of its G matrices replaced by G_λ . Calculating the λ derivative by the Leibniz rule and using [compare with Eq. (14)]

$$\left(\frac{dG_\lambda(W)}{d\lambda}\right)_{\lambda=1} = G(W) + G(W)\mathcal{P}(W)G(W), \quad (\text{A5})$$

we obtain the above mentioned properties at once. These properties can be used to prove the following

Corollary. Assume that the auxiliary potential is defined in the BHF approximation (at least) for hole states. Take any $\langle V \rangle$ diagram \mathcal{V} containing bubbles on hole lines and consider the set \mathcal{S} of diagrams containing \mathcal{V} together with the diagrams one can construct from it by replacing the bubbles by U insertions in all possible ways. Then the total contribution $C_{\mathcal{S}}$ of the diagrams contained in \mathcal{S} vanishes except when \mathcal{V} contains a single bubble and no spurious looking pair. In the latter case, $C_{\mathcal{S}}$ is given by the contribution of \mathcal{V} calculated as if it were an E diagram, i.e., without any extra weighting factor.

Indeed, let n be the number of bubbles on hole lines and p the number of the other G matrices contained in \mathcal{V} . Consider first the case in which \mathcal{V} contains a spurious looking pair. Its contribution $C_{\mathcal{V}}$ is calculated without any extra weighting factor (see property 2) and this also applies to all the other diagrams in \mathcal{S} . Taking into account that the replacement of k bubbles by k U insertions introduces a factor $(-1)^k$, we have

$$C_{\mathcal{S}} = C_{\mathcal{V}} \sum_{k=0}^n (-1)^k \binom{n}{k} = 0, \quad (\text{A6})$$

where $\binom{n}{k}$ is the usual binomial coefficient. Consider now the case in which \mathcal{V} contains no spurious looking pair. Then according to property 3 above, its contribution is given by $(n+p)C_E$ where C_E is the contribution calculated by means of the E -diagram rules. The contribution of a diagram obtained from \mathcal{V} by replacing k bubbles by k U insertions will now be given by $(-1)^k(n+p-k)C_E$. Hence, we have

$$C_{\mathcal{S}} = C_E \sum_{k=0}^n (-1)^k (n+p-k) \binom{n}{k}. \quad (\text{A7})$$

This can be written as

$$C_{\mathcal{S}} = C_E \lim_{x \rightarrow 1} \frac{d}{dx} [x^p (x-1)^n] \quad (\text{A8})$$

which yields

$$\begin{aligned} C_{\mathcal{S}} &= C_E \quad \text{for } n=1 \\ &= 0 \quad \text{for } n>1. \end{aligned} \quad (\text{A9})$$

This completes the proof. The survival of diagram (c) of Fig. 1 illustrates the corollary in a particular case.

[1] *Nuclear Methods and the Nuclear Equation of State*, edited by M. Baldo (World Scientific, Singapore, 1999).
 [2] H. A. Bethe, B. H. Brandow, and A. G. Petscheck, *Phys. Rev.* **129**, 225 (1963).
 [3] B. D. Day, *Phys. Rev. C* **24**, 1203 (1981).
 [4] B. D. Day and R. B. Wiringa, *Phys. Rev. C* **32**, 1057 (1985).
 [5] H. Q. Song, M. Baldo, G. Giansiracusa, and U. Lombardo, *Phys. Rev. Lett.* **81**, 1584 (1998).

[6] B. H. Brandow, *Phys. Rev.* **152**, 863 (1966).
 [7] H. Müther and A. Polls, *Phys. Rev. C* **61**, 014304 (1999).
 [8] B. H. Brandow, *Rev. Mod. Phys.* **39**, 771 (1967).
 [9] K. A. Brueckner and D. T. Goldman, *Phys. Rev.* **117**, 207 (1960).
 [10] G. Baym and C. Pethick, *Landau Fermi-Liquid Theory* (Wiley, New York, 1991).
 [11] C. Mahaux and R. Sartor, *Phys. Rev. C* **19**, 229 (1979).